20th International Congress of Chemical and Process Engineering CHISA 2012
25 – 29 August 2012, Prague, Czech Republic

# Hydrodesulfurization NiMo catalysts supported on Co, Ni and B modified $Al_2O_3$ from Anderson heteropolymolybdates

L. Kaluža[a] a*, R. Palcheva[b], A. Spojakina[b], K. Jirátová[a], G. Tyuliev[b]

[a]Institute of Chemical Process Fundamentals of the ASCR, v.v.i., Prague, Rozvojová 135, 165 02, Czech Republic
[b]Institute of Catalysis, Bulgarian Academy of Sciences, Sofia, acad. G.Bonchev str., bl.11, 1113, Bulgaria

## Abstract

Recent catalysts of hydrodesulfurization (HDS) reaction consist of CoMo and NiMo phase supported on gamma-$Al_2O_3$ support. The support was modified with cobalt nitrate, nickel nitrate, or boric acid and high loadings of Anderson type heteropolyoxomolybdate $(NH_4)_3[Ni(OH)_6Mo_6O_{18}].7H_2O$ were deposited. Surface area ($S_{BET}$) and sulfide phase dispersion of the catalysts were determined by $N_2$ physisorption and $O_2$ chemisorption, respectively. Samples were characterized by X-ray diffraction, X-ray photoelectron spectroscopy, infrared and UV-Vis spectrometry, and temperature programmed reduction. The activity of catalyst was measured in HDS of 1-benzothiophene. The preliminary incorporation of Co, Ni and B into the support increased the HDS activity of the deposited NiMo phase. IR and UV-Vis DR data revealed the partial decomposition of the initial Anderson type NiMo complex with a formation of new surface compounds, including heteropolymolybdates and separated polymeric oxomolybdenum compounds. X-ray photoelectron spectroscopy showed that the degree of Mo sulfidation is the smallest for the catalysts prepared over unmodified alumina and boron-modified alumina. The highest degree of sulfidation was found for the catalysts supported over Co- and Ni-modified alumina. The nickel-modified alumina increased the HDS activity and dispersion of the NiMo phase the most, which was associated with the formation of the largest number of active sites.

*Keywords:* NiMo/γ-$Al_2O_3$; anderson heteropolymolybdate; additives Co, Ni, B; benzothiophene hydrodesulfurization

\* Corresponding author. Tel.: +42-022-039-0293; fax: +42-022-092-0661.
*E-mail address*: kaluza@icpf.cas.cz.

## 1. Introduction

Sulfur compounds present in fuel generate polluting emissions. Increasingly strengthen regulations limits the sulfur content in fuels. Supported Co (Ni) molybdenum catalysts are extensively used in hydrotreating processes for the production of environmentally friendly fuels, and these catalysts have been extensively studied [1]. The nature of the support plays an important role in the morphology and dispersion of the active phases and catalytic activity of the catalysts [2]. A synergistic effect between the support and the NiMo hydrodesulfurization (HDS) catalysts has been proposed [3]. Various supports have been studied for hydrotreating catalysts. The most widely used support remains alumina because of its excellent mechanical and dispersing properties [4]. As a rule, the active components are loaded on the support using cobalt (nickel) nitrates and ammonium heptamolybdate solutions. For this catalyst, the promoting effect of Co(Ni) appears at a Co(Ni)/(Co(Ni)+Mo) ratio of 0.3-0.6 [5]. Despite intensive research over the last decade, the promoting role of Co, Ni, and the support remains unclear. Previous studies have shown that the use of heteropolyoxomolybdate in the preparation of HDS catalysts may provide an interesting alternative to traditional systems [6,7]. It has been shown [8-13] that the usage of ammonium salts (e.g., $CoMo_6O_{24}H_6$ or $NiMo_6O_{24}H_6$) gives a higher HDS activity at a lower Co(Ni)/(Co(Ni)+Mo) molar ratio (0.14). Therefore, Anderson-type heteropolycompounds are effective precursors to the multilayered active phase of hydrotreating catalysts. However, their hydrodesulfurization (HDS) and hydrogenation (HYD) activity depend on the nature of the heteroatom [14].

Various methods of catalyst modification are applied to improve the catalytic performances of the CoMo and NiMo catalysts and to elucidate the effect of the support properties on the HDS activity. Various additives can be used to modify properties of the support. Contradictory results have been reported in the literature regarding their effects on the properties of the alumina support and the HDS catalyst. For example, Li et al. [15] has found a correlation between acidity and HDS activity for the CoMo/alumina-aluminum borate catalysts. They found a beneficial effect on the acidity and metal dispersion upon addition of boron. Ramirez et al. [16] has shown that the promotional effect of boron on HDS activity reaches its maximum at 0.8 wt% B. In contrast, Perez-Martinez et al. [17] has found a decrease in HDS activity based on a study of the effect of acid-base characteristics of alumina ($\gamma$-$Al_2O_3$) modified with B, Na, or K used for diesel hydrotreatment. This result may be due to changes in the distribution of Co and Mo species in the oxide state. Lafitau et al. [18] observed lower interaction between loaded metals and alumina in the presence of boron. On the other hand, Houalla and Delmon revealed that the addition of boron promotes the interaction between cobalt and alumina in the CoMo/$Al_2O_3$ catalysts [19]. Giraldo and Centeno [20] stated that CoMo and NiMo supported on alumina modified by different quantities of $B_2O_3$ (4-14 wt%) did not change the HDS activity at low boron content in these catalysts. The NiMo catalysts showed slightly higher activity than the CoMo catalysts.

Recently we have shown that alumina modified with various amounts of Co prior to the deposition of cobalt heteropolyoxomolybdate up to a molar ratio of Co/Mo = 0.27 substantially increases the activity of the HDS of thiophene and 1-benzothiophene [21]. The aim of this work is to study the influence of Ni, Co or B modification of the alumina support on the properties and the HDS activity of NiMo/$\gamma$-$Al_2O_3$ catalysts prepared using Anderson-type Ni heteropolyoxomolybdate. The activity of the catalysts has been studied for the HDS of 1-benzothiophene.

## 2. Experimental

The parent NiMo catalyst has been prepared using a ground commercial $\gamma$-$Al_2O_3$ support ($S_{BET}$ = 200 $m^2g^{-1}$, total volume of pores = 0.40 $cm^3g^{-1}$, average radius of the pores = 3.2 nm, particle size fraction = 0.16-0.32 mm). The support was impregnated with an aqueous solution of the ammonium salt of nickel

heteropolyoxomolybdate, $(NH_4)4Ni(OH)_6Mo_6O_{18}$ ($NiMo_6$), synthesized according to [22] to obtain a catalyst with 12 wt% of Mo and 1.1 wt% of Ni. Impregnation with nickel heteropolyoxomolybdate was performed in a vacuum evaporator at 70 $^o$C. Then the impregnated support was dried for 4 h at 105 $^o$C and calcined for 2 h at 350 $^o$C. The catalyst is referred to as $NiMo_6$/Al (i.e. unmodified alumina support).

Three other HDS catalysts have been prepared by the addition of $H_3BO_3$, $Co(NO_3)_2$, or $Ni(NO_3)_2$ to the alumina support prior to loading of the $NiMo_6$ salt. First, the alumina support was impregnated with an aqueous solution of the nitrates or boric acid in a vacuum evaporator for 1 h. The modified supports were dried for 4 h at 105 $^o$C and calcined in air for 2 h at 350 $^o$C with a heating rate of 1.7 $^o$C min$^{-1}$. Then the modified supports were impregnated with an aqueous solution of the ammonium salt of nickel heteropolyoxomolybdate and thermally treated for 2 h in air at 350 $^o$C. The catalysts with B, Co and Ni modifications of the alumina support are referred to as $NiMo_6$ /Al-B, $NiMo_6$/Al-Co, and $NiMo_6$/Al-Ni.

The content of transition metals in the catalysts was determined by chemical analysis (Atomic Absorption Spectroscopy). The surface area was determined by nitrogen physisorption at -195 °C using Micromeritics ASAP 2010 after drying the samples at 105 °C and evacuating at 350 °C (approximately 2–5 h). The data were treated by the standard BET method to calculate the specific surface area, $S_{BET}$. The X-Ray measurements were performed using a Bruker AXS 2D Powder X-Ray analyzer with filtered CuKα radiation at 30 kV acceleration with a 10 mA current from the X-Ray tube. Infrared spectra of the samples mixed with KBr at approximately 1 wt% concentration were recorded on a Nicolet 6700 FTIR spectrophotometer (Thermo Fisher Scientific, USA). The spectra were taken in the region of 4000-400 cm$^{-1}$ at 0.4 cm$^{-1}$ resolution using 50 scans. Alumina absorption in the 400-1200 cm$^{-1}$ range was compensated by subtraction of a normalized spectrum of the equivalent amount of support from the spectra of the catalysts. The DR UV-Vis spectra were taken with a Thermo Evolution 300 spectrometer equipped with a Praying Mantis diffuse reflectance accessory.

Temperature-programmed reduction (TPR) measurements of the calcined samples (0.025 g) were performed with an $H_2$/$N_2$ mixture (10 molar% $H_2$) and a flow rate of 50 ml min$^{-1}$ with a linear temperature increase of 20 °C min$^{-1}$ up to 1000 °C [21]. During the TPR measurement, reduction of the grained CuO (0.16-0.315 mm) was performed to calculate the absolute values of the hydrogen consumed during the reduction. Temperature-programmed desorption (TPD) of $NH_3$ was accomplished with a 0.050 g sample at 20-1000 °C with a helium carrier gas and $NH_3$ as an adsorbing gas. Ten doses of ammonia were applied to the catalyst sample at 30 °C before flushing of the sample with helium for 1 h and heating with ramp rate 20 °C min$^{-1}$. The mass contributions (m/z) 2-$H_2$, and 16-$NH_3$ were collected using a Balzers Omnistar mass spectrometer.

Oxygen chemisorption was performed over presulfided catalysts (details on the sulfidation procedure is provided below) flushed by helium (Linde 6.0) at 400 °C for 1 h and cooled in a mixture of dry ice and ethanol. The amount of chemisorbed oxygen was determined from pulses of $O_2$ using a thermal conductivity detector VICI (Valco Instrument Inc., USA) and an HP 3394A integrator (Hewlett Packard).

XPS measurements were performed with an ESCALAB-Mk II (VG Scientific) electron spectrometer with a base pressure of ~5.10-8 Pa. The samples were excited with AlKα radiation (hν = 1486.6 eV). The total energy resolution of the instrument was 1.2 eV as measured by the FWHM of the Ag 3d5/2 photoelectron line. Powdered sulfided samples (details on the sulfidation procedure are provided below) were transferred into their holders without exposure to air in a glove box connected to the fast entry lock of the XPS instrument. The following photoelectron lines were recorded: C 1s, O 1s, Mo 3d, Co 2p, Ni 2p, B 1s, Mo 3p, S 2p. All binding energies were referenced to the C 1s photoelectron line centered at 285.0 eV. The surface atom concentrations were evaluated using the photoelectron peak areas divided by the corresponding sensitivity factors taken from [23].

Hydrodesulfurization of 1-benzothiophene (BT) was performed in the gas phase using an integral fixed-bed tubular flow microreactor (i.d. 3 mm) at 360 °C and 1.6 MPa. Prior to the measurements, the

catalysts were presulfided in situ in a $H_2S/H_2$ flow (1/10) at 400 °C and atmospheric pressure with a temperature ramp of 10 °C min$^{-1}$ and a dwell time of 1 h. The composition of the feed was kept constant at 16 kPa, 200 kPa and 1384 kPa of BT, decane and hydrogen, respectively. The catalyst sample (0.04 g) was diluted with an inert γ-$Al_2O_3$ with particle size fraction 0.16-0.32 mm to form a bed length of 30 mm. To avoid measuring in mass transport mode, the most active catalyst was crushed to particle size fraction 0.08-0.16 mm, diluted with the γ-$Al_2O_3$ and the measurement confirmed that experimental conditions were set up in kinetic mode. The reaction was run at three feed rates of BT including 7.7 mmol h$^{-1}$, 10.3 mmol h$^{-1}$ and 15.5 mmol h$^{-1}$. Steady state was reached in 30 min after each change in the feed rate. Deactivation of the catalysts during the catalytic measurements was not observed. The reaction mixture was analyzed on a Hewlett-Packard gas chromatograph (6890 series) equipped with a capillary column (HP-5, 30 m, 0.53 mm, 1.5 μm). Dihydrobenzothiophene (DH) and ethylbenzene (EB) were identified in the reaction products. The relative compositions ($a_{BT}$, $a_{EB}$ and $a_{DH}$) and conversions ($x_{BT}$, $x_{EB}$, and $x_{DH}$) are defined as $a_{BT} = (1-x_{BT}) = n_{BT}/n_{oBT}$, $a_{EB} = x_{EB} = n_{EB}/n_{oBT}$, $a_{DH} = x_{DH} = n_{DH}/n_{oBT}$, where $n_{oBT}$, $n_{BT}$, $n_{EB}$, and $n_{DH}$ are the initial number of moles of BT, final number of moles of BT, EB, and DH, respectively.

## 3. Results and discussion

### 3.1. Chemical analysis, texture and structure of catalysts

The chemical analysis of the synthesized initial salt (synthesized in our laboratory) showed 46.25 wt% Mo and 4.25 wt% Ni. The molar ratio of Ni/Mo in the initial salt was 0.15. The concentration of Mo in the catalyst was 12 wt%. The catalyst composition is presented in Table 1.

The data presented in Table 1 show a partial reduction of the alumina surface (200 m$^2$ g$^{-1}$) after loading the initial NiMo$_6$ salt. This result can be explained by partial blockage of the mesopores because they contribute most to the $S_{BET}$. However, the modification of γ-$Al_2O_3$ with Co, Ni, and B did not significantly influence the $S_{BET}$ of the NiMo$_6$/Al catalysts. The surface area was slightly higher for the NiMo$_6$/Al-Ni catalyst compared to the others.

Table 1. Composition, specific surface area and porous characteristics of the catalysts.

| Sample | Additive (Ad) (mg g$^{-1}$) | (Ni+Ad)/Mo (mol mol$^{-1}$) | $S_{BET}$ (m$^2$ g$^{-1}$) |
|---|---|---|---|
| γ-$Al_2O_3$ | 0 | - | 200 |
| NiMo$_6$/Al | 0 | 0.15 | 126 |
| NiMo$_6$/Al-Co | 12.60 | 0.31 | 132 |
| NiMo$_6$/Al-B | 12.42 | 1.06 | 123 |
| NiMo$_6$/Al-Ni | 12.48 | 0.32 | 143 |

The XRD patterns of the alumina-supported NiMo catalysts are shown in Fig. 1. Wide-angle X-ray powdered patterns of the NiMo catalysts in their oxidic form were very diffusive. Nevertheless, the diffraction patterns of cubic γ-$Al_2O_3$ with primary 2θ peaks at 46 and 67° could be distinguished in all studied samples. The NiMo$_6$/Al, NiMo$_6$/Al-Co, and NiMo$_6$/Al-B catalysts exhibited the presence of the crystalline orthorhombic phase of $MoO_3$ based on the principal reflection at 27.3°. At given temperatures of calcinations 350 °C it is expected that $MoO_3$, if existing in crystalline form, should occur in

orthorhombic (stable between 330 and 740 $^{o}$C) and probably in monoclinic (stable between 17 and 330 $^{o}$C) structures. However, no crystalline phase of $MoO_3$ was found for the $NiMo_6$/Al-Ni catalyst. The results showed that the Mo superficial species were highly dispersed, either in the form of amorphous particles or as crystallites smaller than 4 nm. The absence of the characteristic reflections of NiO oxides (2θ = 43.5 and 63.0°) in the diffraction pattern of the NiMo catalysts suggested that these compounds were amorphous or microcrystalline.
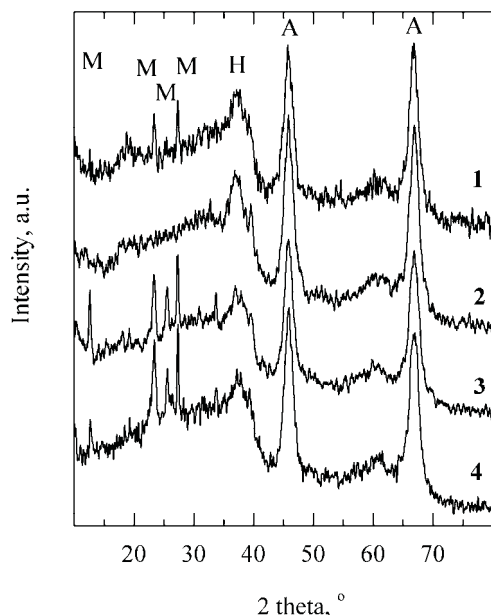


Fig. 1. XRD patterns for the supported $NiMo_6$ catalysts: (1) $NiMo_6$/Al-B, (2) $NiMo_6$/Al-Ni, (3) $NiMo_6$/Al-Co, and (4) $NiMo_6$/Al; identified phases: (M) $MoO_3$, (H) $NiMo_6$ heteropolyoxomolybdates, and (A) $Al_2O_3$.

### 3.2. IR and UV-Vis DRS spectra

The IR spectra of the catalysts prepared by loading Ni heteropolymolybdate onto alumina and alumina modified by Ni, Co or B are shown in Fig. 2 (a). Four broad bands at ca. 440, 650, 890 and 940 cm$^{-1}$ were observed for the unmodified $NiMo_6$/Al catalyst and the three modified catalysts. The IR spectra of the catalysts were very similar but exhibited small differences. According to the literature data, the bands at approximately 440, 650, 890, 940 cm$^{-1}$ are assigned to the vibrations of the Mo-O-Mo bridging bonds ($v_{as}$ = 650 cm$^{-1}$, $v_s$ = 450 cm$^{-1}$) [24] and the bands at 880-950 cm$^{-1}$ correspond to the cis-$MoO_2$ bonds [25]. In the spectra of the samples prepared over modified supports, a small shift in the bands to higher frequencies and a higher ratio of the 890 and 945 cm$^{-1}$ band intensities was observed, especially for the $NiMo_6$/Al-Ni and $NiMo_6$/Al-B catalysts. The increased intensity of the band at 890 cm$^{-1}$ may indicate the formation of $MoO_2$-bonds (i.e. formation of $MoO_3$ particles). The bands at 665 and 945 cm$^{-1}$ (Fig. 2 (a)) may be ascribed to both the partial reaction of the loaded NiMo heteropoly compound with divalent Ni$^{2+}$ ion and the formation of an AlMo compound involving surface aluminum atoms on the support (e.g.

$[AlMo_6O_{24}H_6]^{3-}$). The reaction of the Mo compounds loaded on alumina support has been shown to form aluminum heteropolymolybdate [26]. Accordingly, $Ni^{2+}$ ion can exist in the salt of a new or previously loaded heteropolyanion. In the spectrum of the $NiMo_6$/Al-B sample, the evidence for the $MoO_3$ phase includes higher band intensity at 440 cm$^{-1}$ and shoulders at 823 cm$^{-1}$ and 993 cm$^{-1}$. Ferdous et al. observed similar changes in the FTIR spectra of the $NiMo/Al_2O_3$ catalyst upon addition of 1.7 wt% boron to the catalyst [27].

Fig. 2 (b) represents the electronic spectra of the samples studied, including the initial $NiMo_6$ salt. In the spectra for each of the samples, the bands in the 200 - 350 nm region are characteristic of polymer Mo-O-Mo structures exhibiting charge transfer from $O^{2-}$ to $Mo^{6+}$ with an octahedral coordination. In the low wavelength region of 200 - 400 nm where the contributions of both tetrahedral (Td) and octahedral (Oh) $Mo^{6+}$ appear, only a single broad band with a maximum at approximately 250 nm was present. The broad shape of this charge transfer band, which results from the splitting of two molybdenum states, does not allow for the discrimination between the contributions from Mo(Td) and Mo(Oh) species according to the criteria available in the literature [28].

The appearance of the Mo (Td) band could be associated with the partial disorder of the heteropolyanion structure resulting from the calcination of the samples. Nevertheless, this band was more asymmetric at higher frequencies with nickel and cobalt incorporation, which suggests that a larger portion of the molybdenum has an octahedral coordination induced by these incorporations.
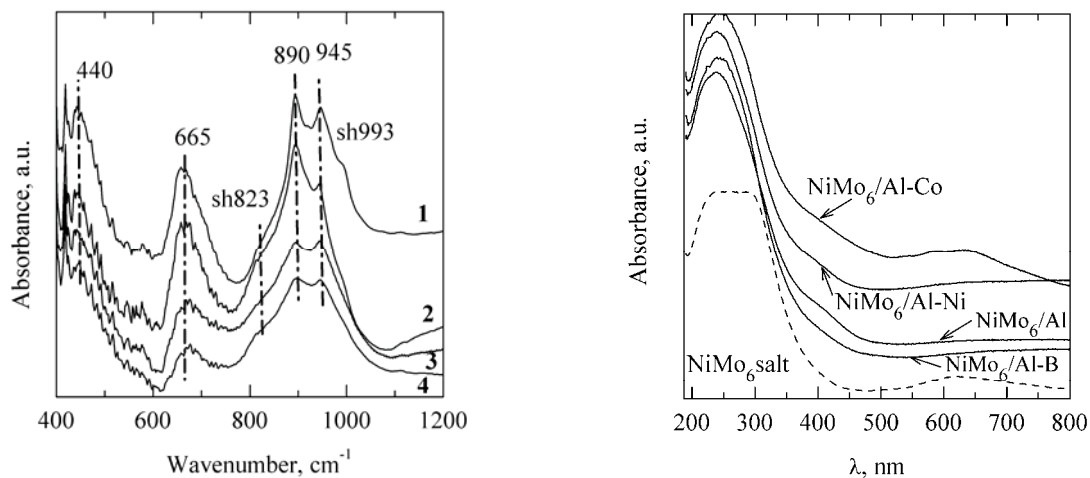


Fig. 2. (a) IR spectra of the calcined NiMo6 catalysts: (1) NiMo6/Al-B, (2) NiMo6/Al-Ni, (3) NiMo6/Al-Co, and (4) NiMo6/Al; (b) UV-Vis DR spectra of the supported NiMo6 catalysts (solid lines) and the original salt (dashed line) [37].

The band around 400 nm was observed for all of these samples and it confirms the presence of octahedral $Ni^{2+}$. The band is overlapped with the strong absorption band of $Mo^{6+}$ (Oh). This band appears as a shoulder in the spectra of the other catalysts. In the spectrum of the initial salt, octahedral $Ni^{2+}$ [29] is also detected at approximately 600-700 nm. In the $NiMo_6$/Al-Co sample, where the modified support was prepared by the loading of cobalt on alumina, a doublet (plateau) appeared in this region (approximately 590 and 640 nm). This plateau is not observed in the spectra of the other catalysts. Therefore, its

appearance results from the addition of cobalt. The band could be assigned to a surface spinel-like phase of $CoAl_2O4$, which is formed during calcination, with tetrahedral $Co^{2+}$, or with octahedral cobalt [30].

### 3.3. TPR and TPD of catalysts

The patterns of the temperature-programmed reduction of the catalysts are presented in Fig. 3 (a). The temperature-programmed reduction of the catalysts was carried out at temperatures up to 1000 °C and revealed three principal peaks for hydrogen consumption (~500, 680 and 920 °C). The peaks with the highest intensity were observed for the $NiMo_6$/Al and $NiMo_6$/Al-Ni catalysts, and the curves for the other two catalysts mainly differ in the high-temperature region (> 500 °C). The reduction profiles correspond to the reduction treatment of the Anderson-type compounds [31]. The change in the signals is due to $Mo^{6+}$ →$Mo^{4+}$ and $Mo^{4+}$→$Mo^0$ reduction processes. The first peak at approximately 450-500 °C can be ascribed to the reduction of $Mo^{6+}$ in the polymeric octahedral Mo species. The other phase ($Mo^{5+}$) simultaneously formed during the reduction reduces to $Mo^{4+}$. The peak observed at approximately 650-700 °C results from the complex reduction process of the present compounds. The addition of nickel to the alumina promotes the reduction of the Mo species that proceeds at a lower temperature where the difference in temperatures is 40 °C (Table 2). This result indicates that, in the $NiMo_6$/Al-Ni sample, the loaded $NiMo_6$ interacts with the Ni-modified alumina forming part of another type of site. It should be noted that the hydrogen consumption observed on the $NiMo_6$/Al-Ni begins at the lowest temperature. This result could be associated with the presence of very small particles on the surface of the catalyst, which is confirmed by the presence of an amorphous phase in the XRD data (Fig. 1). The low-intensity peak at approximately 200 °C appears on the $NiMo_6$/Al-Ni curve, which is most likely associated with the reduction of the highly dispersed $Ni^{2+}$ particles. The modification of the alumina by cobalt only slightly changed the course of the reduction curve for the $NiMo_6$/Al-Co catalyst in comparison to the $NiMo_6$/Al sample.

The TPR curve of $H_2$ consumption for the $NiMo_6$/Al-B sample is different from those of the other catalysts. The first peak appears at a significantly higher temperature compared to the other catalysts. The 547 °C temperature is high enough to reduce $Mo^{6+}$ to $Mo^{4+}$ in the $NiMo_6$/Al-B sample. It is possible that this molybdenum state is more stable in comparison to the other samples, resulting in a significant decrease in the hydrogen consumption for this sample. In addition, we can expect the formation of other reduced species to be more difficult in this sample. The formation of different Mo moieties in the presence of boron has been previously proposed [17]. One Mo moiety, $MoO_3$, was observed in the IR spectrum of this sample (Fig. 2). In this sample, a significant portion of the alumina surface is most likely covered by B atoms. It has been shown that molybdenum forms a weaker bond with B than with Al on the surface of borated alumina [32]. Therefore, bulkier species can be formed during calcination of the sample. Thus, we can expect the formation of other species, which are reduced with more difficulty in this sample. One of these species, $MoO_3$, was observed in the XRD patterns and IR spectrum of this sample (Figs. 1 and 2, respectively).

The highest reduction temperature (approximately 900 °C) observed for all samples can be ascribed to the deep reduction of all of the Mo species formed during the decomposition of the loaded compound and/or to the difficult reduction of tetrahedral Mo-containing species.

The temperature-programmed ammonia desorption (TPD) curves can provide information regarding the concentration and strength of acidic sites in the catalysts. In Fig. 3 (b), ammonia desorption curves observed for all of the prepared catalysts are depicted. Prior to the measurements, the catalysts were calcined for 2 h at 320°C and then heated to 350 °C at a rate of 20° min$^{-1}$.There are no significant differences among the ammonia desorption curves of the examined catalysts. Ammonia desorption starts at approximately 60 °C, reaches a maximum desorption rate at approximately 170-180 °C and then slowly

decreases, reaching a minimum at approximately 1000 °C. The slow decrease in ammonia desorption with increasing temperature reveals the heterogeneity of the strength of the acidic sites. The unmodified $NiMo_6/Al$ catalyst shows a slow and gradual decrease in ammonia desorption similar to the $NiMo_6/Al$-Ni and $NiMo_6/Al$-B catalysts. In contrast, the $NiMo_6/Al$-Co catalysts has a second desorption peak with a maximum at approximately 500 °C, which indicates that this catalyst possesses a slightly higher amount of strong acidic sites compared to the other catalysts. For quantification of the acid properties, we calculated the amount of ammonia desorbed within the range of 25-350 °C because the samples were calcined up to 350 o C prior to the measurements. The results confirm identical amounts of acidic sites (0.56 mmol g$^{-1}$) on the $NiMo_6/Al$ and $NiMo_6/Al$-Co catalysts and slightly higher amounts (0.63 and 0.66 mmol g$^{-1}$) of acidic sites on the $NiMo_6/Al$-Ni and $NiMo_6/Al$-B catalysts, respectively.
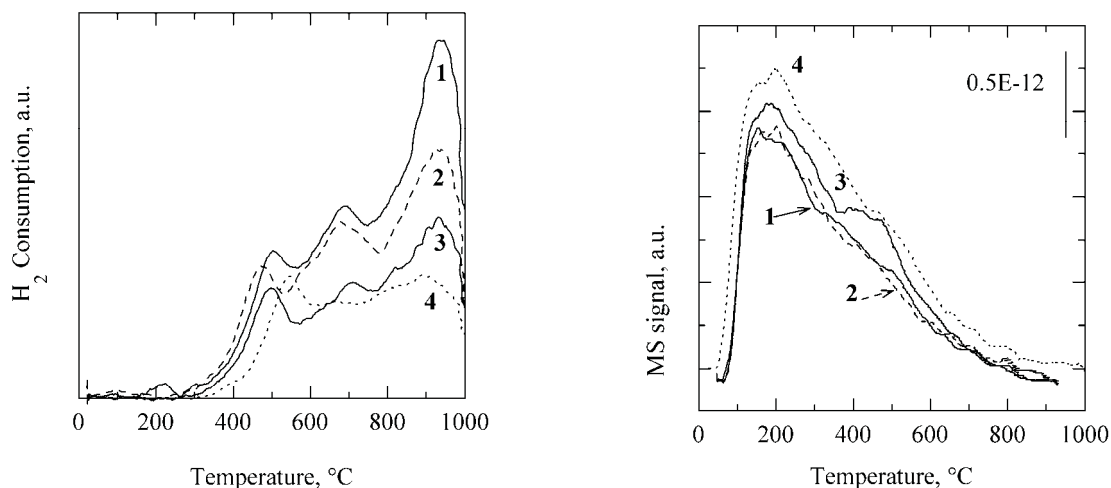


Fig. 3. (a) TPR curves and (b) TPD of ammonia over the HDS catalysts: (1, solid line) $NiMo_6/Al$, (2, dashed line) $NiMo_6/Al$-Ni, (3, solid line) $NiMo_6/Al$-Co, and (4, dotted line) $NiMo_6/Al$-B [37].

### 3.4. XPS results

The oxidation state of the elements in the $NiMo_6$ catalysts prepared over unmodified and modified (Ni, Co, B) γ-alumina support were examined using XPS for both the calcined and sulfided form. The spectra of the calcined catalysts possess Mo 3d and Ni 2p features that are characteristic of $Mo^{6+}$ and $Ni^{2+}$ in an oxide matrix. The binding energy of $Mo^{6+}$ that corresponds to Mo 3d$_{5/2}$ is 232.8 eV, and the binding energy of $Ni^{2+}$ that corresponds to Ni 2p$_{3/2}$ is 856.3 eV. The binding energies of the other important catalyst components are as follows: Co 2p$_{1/2}$ = 797.2 eV (792.9 eV for the sulfided catalyst), Al 2p = 75.0 eV, B 1s = 192.8 eV (192.5 eV for the sulfided catalyst), S 2p$_{3/2}$ = 162.0 eV and O 1s = 531.5 eV. Surface atom ratios (Mo/Al, Ni/Al, Co/Al, B/Al and S/Al) determined for the catalysts prepared in the calcined and sulfided states are shown in Table 2. The Mo/Ni intensity ratio for the calcined $NiMo_6/Al$ and $NiMo_6/Al$-Co catalysts is slightly lower (5.48 and 5.84, respectively) than the stoichiometric value

expected for $NiMo_6$ heteropoly compounds. A significantly lower Mo/Ni intensity ratio (Mo/Ni 2.85) was found for the calcined NiMo6/Al-Ni catalyst because of the modification of the alumina support by nickel. After sulfidation of the catalysts, the Mo/Ni intensity ratios increased slightly for the $NiMo_6$/Al and $NiMo_6$/Al-B catalysts and decreased for the $NiMo_6$/Al-Co and $NiMo_6$/Al-Ni catalysts. The observed changes in the surface layer of the catalyst could indicate decomposition of the $NiMo_6$ heteropoly compound and formation of bulky Mo species on the catalyst surface during sulfidation.

Table 2. Surface atom ratios for the $NiMo_6$ catalysts as derived from the XPS data (photoelectron lines used in the quantification are also indicated) and the degree of metal oxide sulfidation.

| Sample | Surface Atomic Ratio | | | | | | | Degree of metal oxide sulfidation (%) | | |
|---|---|---|---|---|---|---|---|---|---|---|
| | Mo/Al | Mo/Al | Ni/Al | B/Al | Co/Al | Mo/Ni | S/Al | | | |
| | Mo 3d, Al 2p | Mo 3p, Al 2p | Ni 2p, Al 2p | B 1s, Al 2p | Co 2p, Al 2p | Mo 3d, Ni 2p | S 2p, Al 2p | Mo 3d | Ni $2p_{3/2}$ | Co $2p_{1/2}$ |
| Calcined | | | | | | | | | | |
| $NiMo_6$/Al | 0.074 | 0.071 | 0.0135 | 0 | 0 | 5.48 | 0 | 0 | 0 | - |
| $NiMo_6$/Al-Co | 0.089 | 0.086 | 0.0153 | 0 | 0.0268 | 5.84 | 0 | 0 | 0 | 0 |
| $NiMo_6$/Al-B | 0.117 | 0.112 | 0.0195 | 0.0445 | 0 | 6.01 | 0 | 0 | 0 | - |
| $NiMo_6$/Al-Ni | 0.088 | 0.092 | 0.0310 | 0 | 0 | 2.85 | 0 | 0 | 0 | - |
| Sulfided | | | | | | | | | | |
| $NiMo_6$/Al | 0.081 | 0.078 | 0.0120 | 0 | 0 | 6.77 | 0.062 | 31 | 43 | - |
| $NiMo_6$/Al-Co | 0.093 | 0.091 | 0.0178 | 0 | 0.0293 | 5.23 | 0.156 | 61 | 83 | 25 |
| $NiMo_6$/Al-B | 0.109 | 0.110 | 0.0144 | 0.0504 | 0 | 7.55 | 0.119 | 47 | 43 | - |
| $NiMo_6$/Al-Ni | 0.072 | 0.076 | 0.0275 | 0 | 0 | 2.61 | 0.169 | 71 | 57 | - |

In the sulfided catalysts, new spectral features were observed in the Mo 3d, Ni 2p and Co 2p photoelectron lines corresponding to metal sulfide phases. The Mo 3d spectra for the sulfided $NiMo_6$ catalysts were decomposed into two main components (i.e. $Mo^{4+}$ and $Mo^{6+}$) because three components decomposition (i.e. $Mo^{4+}$, $Mo^{5+}$ and $Mo^{6+}$) led to low level of $Mo^{5+}$ over all studied samples. The first component corresponds to the sulfide state with Mo $3d_{5/2}$ at $229.0\pm0.1$ eV ($Mo^{4+}$), and the second one corresponds to Mo $3d_{3/2}$ at 232.6 eV ($Mo^{6+}$), which represents the $Mo^{6+}$ in the calcined samples. As can be seen from Table 3 and Fig. 6, the degree of Mo sulfidation expressed by the ratio of $Mo^{4+}/(Mo^{4+} + Mo^{6+})$ is the smallest for the catalysts prepared over unmodified alumina and boron modified alumina. On the other hand, the highest degree of sulfidation was found for the catalysts supported over Co- and Ni-modified alumina. In addition, the occurrence of $Mo^{6+}$ in the surface layer is lower for $NiMo_6$ catalysts prepared over modified alumina (Table 2).

The decomposition of the Ni $2p_{3/2}$ line for all of the sulfided $NiMo_6$ catalysts, the Co $2p_{1/2}$ line for the $NiMo_6$/Al-Co catalyst and the Mo 3d lines for the sulfide catalysts resulted in two components. The first component with Ni $2p_{3/2}$ (main line) at $853.4\pm0.2$ eV is attributed to $Ni^{2+}$ in the sulfided form, and the second one located at 856.4 eV is ascribed to the unsulfured Ni. For cobalt, the binding energies were as follows: 792.9 eV for $Co^{2+}$ in a sulfided form and 797.2 eV for $Co^{2+}$ in the oxidic form. The surface concentration of Ni in the sulfided unmodified catalyst and $NiMo_6$/Al-B catalysts is lower than the

concentration in the corresponding calcined catalysts (Table 2). In contrast, the surface concentration of Ni in the sulfided $NiMo_6$/Al-Co and $NiMo_6$/Al-Ni catalysts was higher than that found for their calcined counterparts. The degree of nickel sulfidation is 43 % for the catalysts prepared over unmodified and B-modified alumina. The degree of sulfidation of nickel in the remaining catalysts, $NiMo_6$/Al-Co and $NiMo_6$/Al-Ni, was substantially higher, 83 and 57 %, respectively.

In summary, we did not observe significant change in the Ni/Al intensity ratio after catalyst sulfidation. Therefore, the Ni particles on the catalyst surface exist in a multilayer structure and are partly shadowed by the $MoS_2$ slabs [33]. An increase in the Mo/Al ratio was observed for the oxidic and sulfided $NiMo_6$ catalysts supported on modified aluminas, especially for the oxidic $NiMo_6$/Al-B catalyst (Table 3). The formation of a borate monolayer on the alumina surface has been reported by Maity et al. [34]. Therefore, a higher production of the $MoS_2$ phase in the $NiMo_6$/Al-B catalyst can be expected.

### 3.5. HDS of 1-benzothiophene and sulfide phase dispersion

The activity of the catalysts in HDS reaction of 1-benzothiophene was expressed as the empirical pseudo-first-order rate constants of benzothiophene consumption ($k_{BT}$) and of ethylbenzene formation ($k_{EB}$). The HDS activities ($k_{BT}$s and $k_{EB}$s) of the prepared catalysts are compared with the sulfide phase dispersion represented by the amount of chemisorbed oxygen in Table 3. Both empirical activity indexes ($k_{BT}$ and $k_{EB}$) possessed similar values because the formation of dihydrobenzothiophene (i.e. the product of benzothiophene hydrogenation) was extremely low over all of the studied catalyst. This is quite typical for the NiMo phase [35]. Modification of the support with Co, Ni, or B increased the activity of the $NiMo_6$ phase by approximately 1.3-2.3 fold (based on weight-normalized activities) or 1.2-2.0 fold (based on intrinsic activities). Furthermore, the activities correlated well with the amount of chemisorbed oxygen. Clearly, the $NiMo_6$/Al-Ni catalyst exhibited the highest dispersion and HDS activity, which was comparable with the previously reported activity of industrial catalysts [21]. Despite the formation of dihydrobenzothiophene being extremely low over all of the studied catalysts, there were differences found for the selectivities, which are expressed as C=C hydrogenation/C-S hydrogenolysis. The selectivity to dihydrobenzothiophene is shown in Fig. 4. The most active catalyst, $NiMo_6$/Al-Ni, exhibited the lowest selectivity to dihydrobenzothiophene (Fig. 4). The modification of the support by Ni resulted not only in a significant increase in the quantity of active sites formed from the deposited $NiMo_6$ (i.e., the dispersion by chemisorbed $O_2$) but also an increase in the quality of the active sites (i.e. the lowest selectivity to DH). XPS results also revealed that the $NiMo_6$/Al-Ni catalyst had the highest surface Ni concentration and the highest degree of active sulfided components.

A comparison of the catalytic activities in Table 3 indicates a positive effect from the modification of alumina support by additive ions (Ni, Co or B). The highest activity for 1-benzothiophene hydrodesulfurization was observed with the $NiMo_6$ catalyst that was prepared over alumina modified with nickel. A similar effect of support modification on the activity for the HDS of thiophene and 1-benzothiophene was observed with the CoMo catalysts prepared by loading heteropolymolybdate on alumina modified with cobalt [21]. Furthermore, it was previously found that this preparation method led to stable and active catalyst in gas oil hydrodesulfurization performed in a pilot plant [36]. Because a good correlation between the model HDS of 1-benzothiophene and HDS of gas oil was observed [36], the prepared $NiMo_6$/Al-Ni catalyst was identified as a relevant candidate for further investigation in a pilot plant scale HDS.

Table 3. HDS activity and chemisorbed $O_2$.

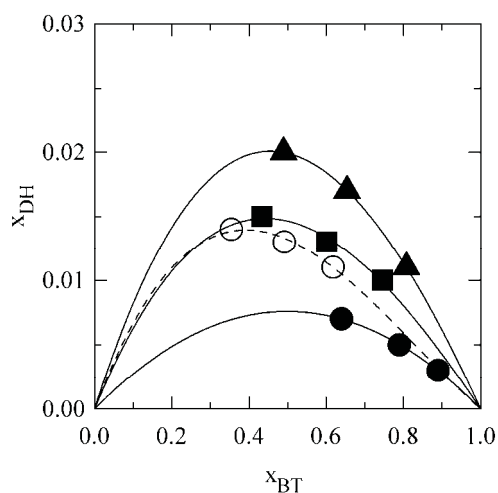| Catalysts | $k_{EB}$ mmol $g^{-1}.h^{-1}$ | $k_{BT}$ mmol $g^{-1}.h^{-1}$ | $O_2$ mmol $g^{-1}$ |
|---|---|---|---|
| NiMo$_6$/Al | 171 | 178 | 12 |
| NiMo$_6$/Al-Co | 233 | 241 | 15 |
| NiMo$_6$/Al-B | 270 | 282 | 15 |
| NiMo$_6$/Al-Ni | 398 | 404 | 28 |

Fig. 4. Selectivity to dihydrobenzothiophene (DH) during benzothiophene (BT) hydrodesulfurization: (open circle, dashed line) NiMo$_6$/Al, (squares, solid line) NiMo$_6$/Al-Co, (filled triangles, solid line) NiMo$_6$/Al-B, and (filled circle, solid line) NiMo$_6$/Al-Ni [37].

## 4. Conclusion

The alumina-supported NiMo hydrodesulfurization catalysts have been prepared by loading the Anderson-type nickel heteropolyoxomolybdate on the alumina initially modified with nickel, cobalt or boron. Nickel incorporation in the alumina prior to loading the NiMo$_6$/Al-Ni catalyst (molar ratio of the total amount Ni in the catalysts is Ni/(Mo+Ni) = 0.24) resulted in an activity for 1-benzothiophene hydrodesulfurization that was nearly twice as much as the activity observed for the NiMo$_6$/Al, NiMo$_6$/Al-B and NiMo$_6$/Al-Co catalysts. The IR results confirm the stability of the heteropolymolybdate structure in the calcined catalysts. A mixture of initial and aluminum heteropolymolybdates are present in the catalysts. The highest activity observed for the Ni-modified catalyst is primarily associated with the formation of the largest number of active sites.

## Acknowledgements

## References

[1] Topsoe H, Clausen BS, Massoth F E. *Hydrotreating Catalysis: Science and Technology*. Berlin: Springer-Verlag, 1996.

[2] Breysse M, Afanasiev P, Geantet C, Vrinat M. *Catal Today* 2003;**86** 5-16.

[3] Laine J, Severino F, Labady M, Gallardo J. *J Catal* 1992;**138** 145-9.

[4] Chorkendorff I, Niemantsverdriet JW. *Concept of Modern Catalysis and Kinetics*. Weinheim: Wiley-VCH Verlag, 2007.

[5] Chianelli R, Daage M, Ledoux M J. *Adv Catalysis* 1994;**40**:177-232.

[6] Spozhakina A, Kostova N, Yuchnovski I, Shopov D, Yurieva T, Shokhireva T. *Appl Catal* 1988;**39**:333-342.

[7] Griboval A, Blanchard P, Gengembre L, Payen E, Faurnier M, Dubois L, et al. *J Catal* 1999; **188**:102-110.

[8] Spojakina A, Gigov B, Shopov DM. *React Kinet Catal Lett* 1982;**19**:11-4.

[9] Carrier X, Lambert JF, Che M. *J Am Chem Soc* 1997;**119**:10137-46.

[10] Cabello CI, Botto I, Thomas HJ. *Appl Catal A: Gen* 2000;**197**: 79-86.

[11] Cabello CI,. Botto IL, Gabrerizo F, Gonzalez MG, Thomas HJ. *Ads Sci Technol* 2000;**18**:591-608.

[12] Pettiti I, Botto IL, Cabello CI, Colonna S, Fatticanti M, Minelli G, et al. *Appl Catal A: Gen* 2001;**220**:113-121.

[13] Spojakina A, Kraleva E, Jiratova K. *Kinetics and Catalysis* 2010;**51**:385-93.

[14] Nikulshin PA, Tomina NN, Pimerzin AA, Stakheev AY, Mashkovsky IS, et al. *Appl Catal A: Gen* 2011;**393**:146-152.

[15] Li C, Chen YW, Yang SJ, Wu JC. *Ind Eng Chem Res* 1993;**32**:1573-8.

[16] Ramirez J, Castillo P, Cedefio L, Cuevas R, Castillo M, Palacios JM, et al. *Appl Catal A: Gen* 1995;**132**:317-34.

[17] Perez-Martinez DJ, Eloy P, Gaigneaux EM, Giraldo SA, Centeno A. *Appl Catal A: Gen* 2010;**390**:59-70.

[18] Lafitau H, Neel E, Clement JC. *Stud Surf Sci Catal* 1976;**l**:393-404.

[19] Houalla M, Delmon B. *Appl Catal* 1981;**1**:285-9.

[20] Giraldo SA, Centeno A. *Catal Today* 2008;**133-135**:255-60.

[21] Palcheva R, Spojakina A, Jiratova K, Kaluža L. *Catal Lett* 2010;**137**:216-23.

[22] Nomiya K, Takahashi T, Shirai T, Miwa M. *Polyhedron* 1987;**6**:213-8.

[23] Scofield JH. *J Electron Spectrosc Relat Phenom* 1976;**8**:129-37.

[24] Davydov AA, Goncharova OI. *Russ Chem Review* 1993;**62**:105-20.

[25] Yurchenko EN. *Molecular Spectroscopy in the Chemistry of Coordination Comp. and Catalysts*. Novosibirsk: Nauka; 1986.

[26] Goncharova OI, Boreskov GK, Yurieva TM, Yurchenko EN, Boldyreva NN. *React Kinet Catal Lett* 1981;16:349-53.

[27] Ferdous D, Dalai AK, Adjaye J. *Appl Catal A: Gen* 2004;**260**:137-51.

[28] Fournier M, Louis C, Che M, Chaquin P, Masure D. *J Catal* 1989;**119**:400-14.

[29] Porta P, Stone FS, Turner RG. *J Solid State Chem* 1974;**11**:135-47.

[30] Gajardo P, Grange P, Delmon B. *J Catal* 1980;**63**:201-16.

[31] Botto LL, Cabello CI, Thomas HJ, Cordisc D, Minelli G, Porta P. *Mater Chem Phys* 2000;**62**:254-62.

[32] Saih Y, Segawa K. *Appl Catal A: Gen* 2009;**353**:258-65.

[33] Bouwens SMAM, Vanzon FBM, Vandijk MP, Vanderkraan AM, Debeer VHJ, et al. *J Catal* 1994;**146**:375-93.

[34] Maity SK, Lemus M, Ancheyta J. *Enery and Fuels* 2011;**25**:3100-7.

[35] Kaluža L, Gulková D, Šolcová O, Žilková N, Čejka J. *Appl Catal A: Gen* 2008;**351**:93-101.

[36] Spojakina A, Jirátová K, Novák V, Palcheva R, Kaluža L. *Collect Czech Chem Commun* 2008;**73**:983-99.

[37] Palcheva R, Kaluža L, Spojakina A, Jirátová K, Tyuliev G. *Chinese J Catal* submitted.